THE JOURNAL OF PHYSICAL CHEMISTRY LETTERS
A JOURNAL OF THE AMERICAN CHEMICAL SOCIETY

Open Access
This article is licensed under CC-BY 4.0

pubs.acs.org/JPCL
Letter

Disorder in Order-Related Membrane Biophysical Parameters: An In-Depth Analysis of Di-4-ANEPPDHQ Generalized Polarization

Rosemary Chandrakanthi Kothalawala, Csenge Makay, Lajos Szente, Zoltan Varga, Gyorgy Panyi, Peter Nagy, Florina Zakany,* and Tamas Kovacs*

Cite This: J. Phys. Chem. Lett. 2026, 17, 4723−4731

Read Online

ACCESS | Metrics & More | Article Recommendations | Supporting Information

ABSTRACT: Molecular order-related bulk membrane properties that substantially modulate protein functions can be examined with environment-sensitive probes, such as the prototypical and most widely applied solvatochromic Laurdan, whose spectral parameters change depending on the local hydrophobicity. Di-4-ANEPPDHQ is a widely accepted Laurdan alternative with more favorable spectral properties suitable for standard imaging, and information provided by the two fluorophores is generally considered equivalent. In our study, using fluorescence-based experimental approaches, we demonstrate that different sterols distinctly alter di-4-ANEPPDHQ spectral properties, and these changes do not correlate with those observed with Laurdan. Our molecular dynamics simulations reveal that this may be caused by their distinct depth localization in bilayers since the sensor moiety of di-4-ANEPPDHQ is localized in the vicinity of the membrane−water interface as opposed to that of Laurdan lying near the hydrophobic core. Therefore, di-4-ANEPPDHQ can be considered as a complementary tool rather than an equivalent substitute of Laurdan.

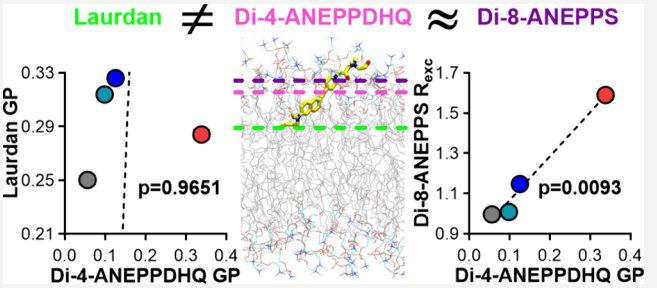

Downloaded via UNIV OF DEBRECEN on May 11, 2026 at 11:10:10 (UTC).
See https://pubs.acs.org/sharingguidelines for options on how to legitimately share published articles.

The bulk structural organization is an essential, intrinsic, and dynamic property of all biological membranes, which plays a fundamental active role in the modulation of membrane protein activity and, therefore, a wide variety of cellular functions.[1,2] However, examination of such membrane features is often neglected in the new era of cutting-edge structural techniques, such as X-ray crystallography or cryoelectron microscopy, in studies of protein structures and direct lipid−protein interactions, which is also partially attributable to the scarcity of experimental methods suitable for the investigation of membrane organization in living cells. For this purpose, environment-sensitive fluorophores can be utilized in intact cells, which change their fluorescence properties in response to alterations in the local microenvironment. These dyes are routinely classified based on the mechanism of sensitivity with the largest families comprising viscosity-sensitive fluorescent probes, polarity-sensitive solvatochromic dyes, and voltage-sensitive electrochromic dyes.[3,4] These major groups of probes characterize three different aspects of molecular organization in the membrane, i.e., membrane fluidity, hydration, and dipole potential, respectively. From among these order-related parameters, fluidity is defined as the rotational freedom of molecules, hydration is defined as the extent of penetration of water into the bilayer, whereas dipole potential represents a large positive intramembrane potential arising from the nonrandom orientation of molecular dipoles at the membrane−water interface.[5−9] Since these properties are essentially linked to each other, they are often collectively termed "membrane order" or "lipid order" and results obtained with the different environment-sensitive dyes are considered equivalent in spite of sporadic results demonstrating incongruent changes in the fluorescence properties of the dyes in response to alterations in membrane lipid composition.[10−12] In accordance with the latter, in our previous study with fluorescence-based experimental approaches, we demonstrated dissimilar changes in the fluorescence properties of four commonly applied environment-sensitive dyes elicited by different sterols, and using molecular dynamics simulations, we showed that the distinct sensitivity of the dyes is caused by the incorporation of their sensor moieties at different bilayer depths.[13]

Solvatochromic dyes are frequently utilized to describe molecular order in membranes, and Laurdan (6-dodecanoyl-*N*,*N*-dimethyl-2-naphthylamine) is the founding prototypical member of the family since its emission spectrum is altered as a function of the local hydrophobicity.[14,15] Namely, its emission spectrum is red-shifted in a hydrophilic environment due to solvent relaxation, i.e., a rapid reorganization of water

Received: January 7, 2026
Revised: March 12, 2026
Accepted: March 13, 2026
Published: April 10, 2026

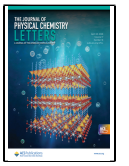

ACS Publications
© 2026 The Authors. Published by American Chemical Society

https://doi.org/10.1021/acs.jpclett.6c00048
J. Phys. Chem. Lett. 2026, 17, 4723−4731

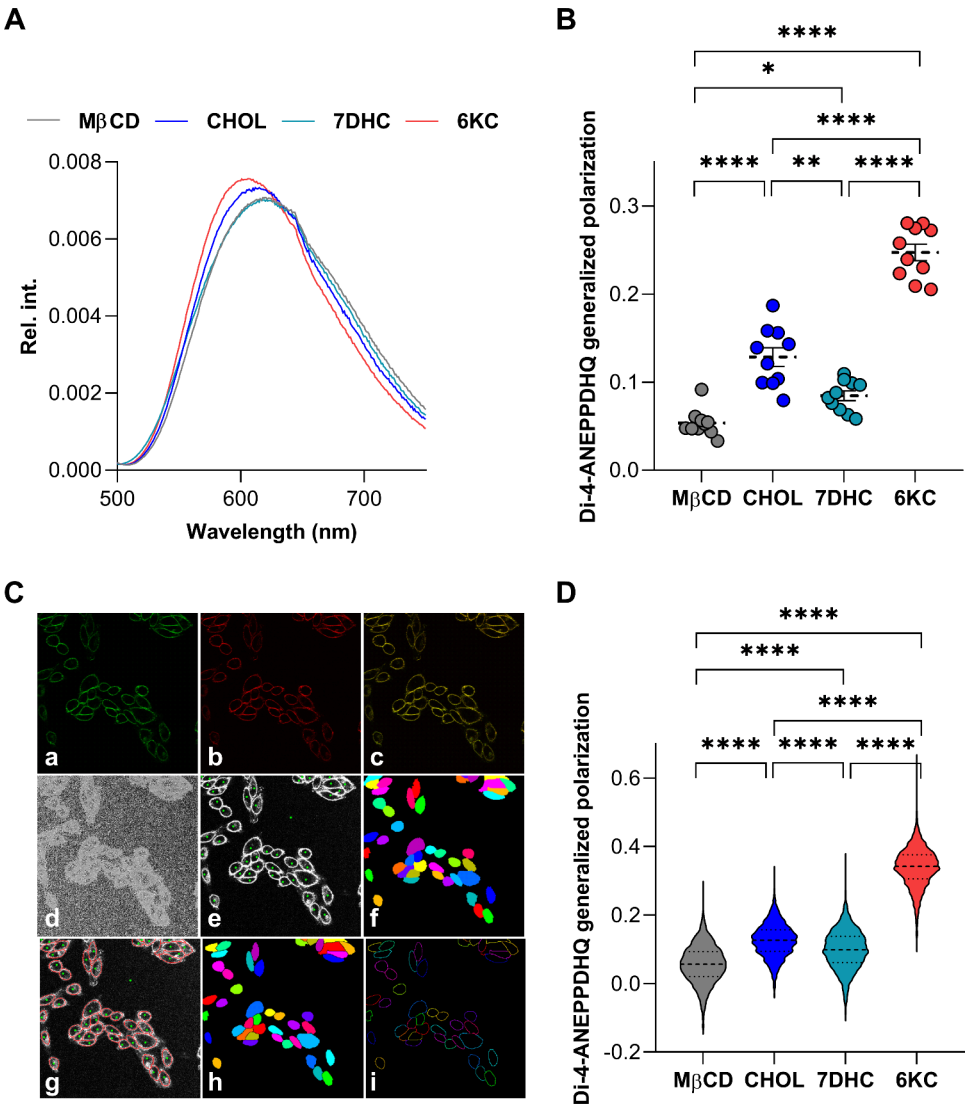

Figure 1. Effects of cyclodextrin-complexed sterols on the generalized polarization of di-4-ANEPPDHQ. (A) Detached CHO cells were treated for 1 h with native MβCD and cholesterol−MβCD (CHOL), 7-dehydrocholesterol−MβCD (7DHC), and 6-ketocholestanol−MβCD (6KC) complexes and stained with di-4-ANEPPDHQ. Emission spectra were acquired after a 488 nm excitation using spectrofluorometry. (B) Individual di-4-ANEPPDHQ generalized polarization values were subsequently obtained from the spectra in n = 10 independent samples containing approximately 100 000 cells, and their average values (±SEM) are plotted in the figure. (C) CHO cells grown on an eight-well chambered coverglass were treated and stained as described above. Representative confocal microscopic images taken at the midplane of cells show di-4-ANEPPDHQ intensities measured in the (a) blue and (b) red wavelength ranges, and (c) their overlay. During quantitative image analysis, (d) the generalized polarization was calculated on a pixel-by-pixel basis and (e) a custom-written manually seeded watershed algorithm was applied to identify (f) the cells and (g) the pixels corresponding to the plasma membrane of cells. (h) This was followed by the identification of individual cells and, consequently, (i) plasma membrane pixels of individual cells. (D) Violin plots were generated from median di-4-ANEPPDHQ generalized polarization values calculated exclusively from pixels corresponding to the plasma membrane in n = 3500−4000 individual cells per treatment condition obtained from five independent experiments, which also display median values with quartiles. Asterisks indicate significant differences between the samples (*p < 0.05, **p < 0.01, and ****p < 0.0001; ANOVA followed by Tukey's HSD test).

molecules in the vicinity thereby decreasing the energy of the excited state. The generalized polarization of the probe quantifying the extent of this spectral shift thus negatively correlates with the degree of water penetration into the membrane, and its quantification is widely utilized in living cells to report on membrane structure.[10,11,16−20] However, its applicability is limited by its unfavorable spectral properties; in other words, its excitation spectrum falls in the near-UV range. Therefore, the generalized polarization of Laurdan is typically determined with spectrofluorometry, which lacks the ability to provide information about individual cells[10,11,17] or two-photon microscopy, which is not widely available.[16,18,20,21]

Di-4-ANEPPDHQ was introduced as an environment-sensitive probe having more favorable, red-shifted spectra suitable for imaging with conventional microscope setups.[22,23] Upon examination in combination with Laurdan, the two fluorophores gave similar results, and consequently, di-4-ANEPPDHQ became accepted as a Laurdan alternative to characterize membrane structure.[19,24−30] However, sporadic results showed that the information provided by the two dyes is not necessarily equivalent, and therefore, di-4-ANEPPDHQ cannot be considered as a full-fledged alternative of Laurdan.[31,32] In our study, using fluorescence-based approaches, we also provide evidence that the two dyes may

https://doi.org/10.1021/acs.jpclett.6c00048
J. Phys. Chem. Lett. 2026, 17, 4723−4731

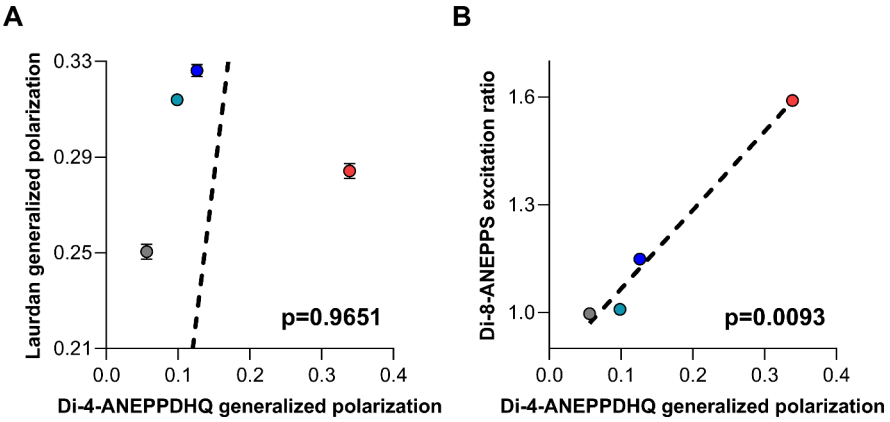

Figure 2. Comparison of the effects of cyclodextrin-complexed sterols on the generalized polarization of di-4-ANEPPDHQ, the generalized polarization of Laurdan, and the excitation ratio of di-8-ANEPPS. (A) Laurdan generalized polarization plotted as a function of di-4-ANEPPDHQ generalized polarization. (B) Di-8-ANEPPS excitation ratio plotted as a function of di-4-ANEPPDHQ generalized polarization. Average values (±SEM) of the Laurdan generalized polarization and di-8-ANEPPS excitation ratio, determined in our previous study[13] under identical experimental conditions, are compared with di-4-ANEPPDHQ generalized polarization values measured in the present study in cells treated with native MβCD (gray) and cholesterol−MβCD (CHOL, dark blue), 7-dehydrocholesterol−MβCD (7DHC, cyan), and 6-ketocholestanol−MβCD (6KC, red) complexes. The *p* values determined with Deming regression analysis are shown in the panels, which revealed a significant correlation only between the di-4-ANEPPDHQ generalized polarization and di-8-ANEPPS excitation ratio.

exhibit incongruent responses due to, as revealed by our molecular dynamics simulations, distinct depth localization in bilayers.

The structural organization and therefore the biophysical properties of bilayers substantially depend on the quality and quantity of membrane lipids. Membrane cholesterol is one of the major determinants of membrane structure since its concentration negatively correlates with membrane fluidity[12,17,33,34] and hydration[12,17−19,25,35] through inducing the stretching of acyl chains of phospholipids, altering penetration and ordering of membrane-associated water molecules. Due to these same membrane-ordering properties, the cholesterol concentration positively correlates with the dipole potential.[10,12,36−41] Other sterols also modify membrane organization but often in a distinct manner. For example, 7-dehydrocholesterol similarly reduces fluidity and hydration[12,42] by inducing smaller increases in the dipole potential.[12,37,43] Conversely, 6-ketocholestanol largely increases the dipole potential[10,12,44−46] without causing notable changes in fluidity or hydration.[10,12] The altered effects on the membrane structure of these sterols may be related to distinct magnitudes of their dipole moment, tilt angles in the bilayer, different depth localization in the membrane, and effects on penetration and ordering of membrane-associated water molecules.

Due to the uncertainty regarding which membrane biophysical property di-4-ANEPPDHQ reports, the aim of this work is to correlate its response to cholesterol analogues with that of Laurdan (a probe of membrane hydration) and di-8-ANEPPS (a reporter of dipole potential). Changing the levels of cholesterol, 7-dehydrocholesterol, and 6-ketocholestanol induces distinct alterations in membrane structure, which enables studying the sensitivity of environment-sensitive fluorophores to different aspects of membrane organization as performed in our previous study.[13] These sterols can be experimentally incorporated into the membranes by using their inclusion complexes with randomly methylated β-cyclodextrin (MβCD). In native empty form, MβCD depletes membrane cholesterol, whereas when precomplexed, it can efficiently load bilayers with sterols.[5,12,43,47,48] However, precomplexation results in a mixture of empty and sterol-loaded MβCD, and as a result, two competing processes occur during treatment of cells, that is, cholesterol depletion and sterol loading. Therefore, MβCD-treated samples should serve as controls in these experiments.[12,43,48]

In accordance, to examine effects on di-4-ANEPPDHQ generalized polarization, we treated CHO cells with MβCD precomplexed with cholesterol (CHOL), 7-dehydrocholesterol (7DHC), and 6-ketocholestanol (6KC) and empty MβCD as a control. After treatment and thorough washing, we labeled the cells with di-4-ANEPPDHQ and followed changes in the emission spectrum of the dye using spectrofluorometry. In these experiments, we observed blue-shifts in the spectrum in response to all three sterols when compared to the control, implying a more hydrophobic microenvironment, that is, less membrane hydration (Figure 1A). However, the degree of shifts was notably different among the sterols. We determined the extent of these shifts by calculating the generalized polarization, and significant increases were found when comparing each sterol to the control and between the sterols, as well, with values for the different treatments decreasing in the following order: 6KC ≫ CHOL > 7DHC > MβCD (Figure 1B). Since spectrofluorometry does not provide information about individual cells and the main advantage of di-4-ANEPPDHQ over Laurdan is its suitability for conventional imaging, we performed these measurements with confocal microscopy, as well. During quantitative image analysis, we identified individual cells and calculated the median value of generalized polarization exclusively in the plasma membranes of individual cells (Figure 1C). We found strongly concordant results with those seen using spectrofluorometry with di-4-ANEPPDHQ generalized polarization values in the following order: 6KC ≫ CHOL > 7DHC > MβCD (Figure 1D).

In the next step, we compared our results with those obtained in our previous study after identical treatments and experimental conditions with solvatochromic Laurdan and electrochromic di-8-ANEPPS.[13] We performed Deming regression analysis between di-4-ANEPPDHQ generalized polarization and Laurdan generalized polarization or di-8-ANEPPS excitation ratio values obtained after MβCD, CHOL,

https://doi.org/10.1021/acs.jpclett.6c00048
J. Phys. Chem. Lett. 2026, 17, 4723−4731

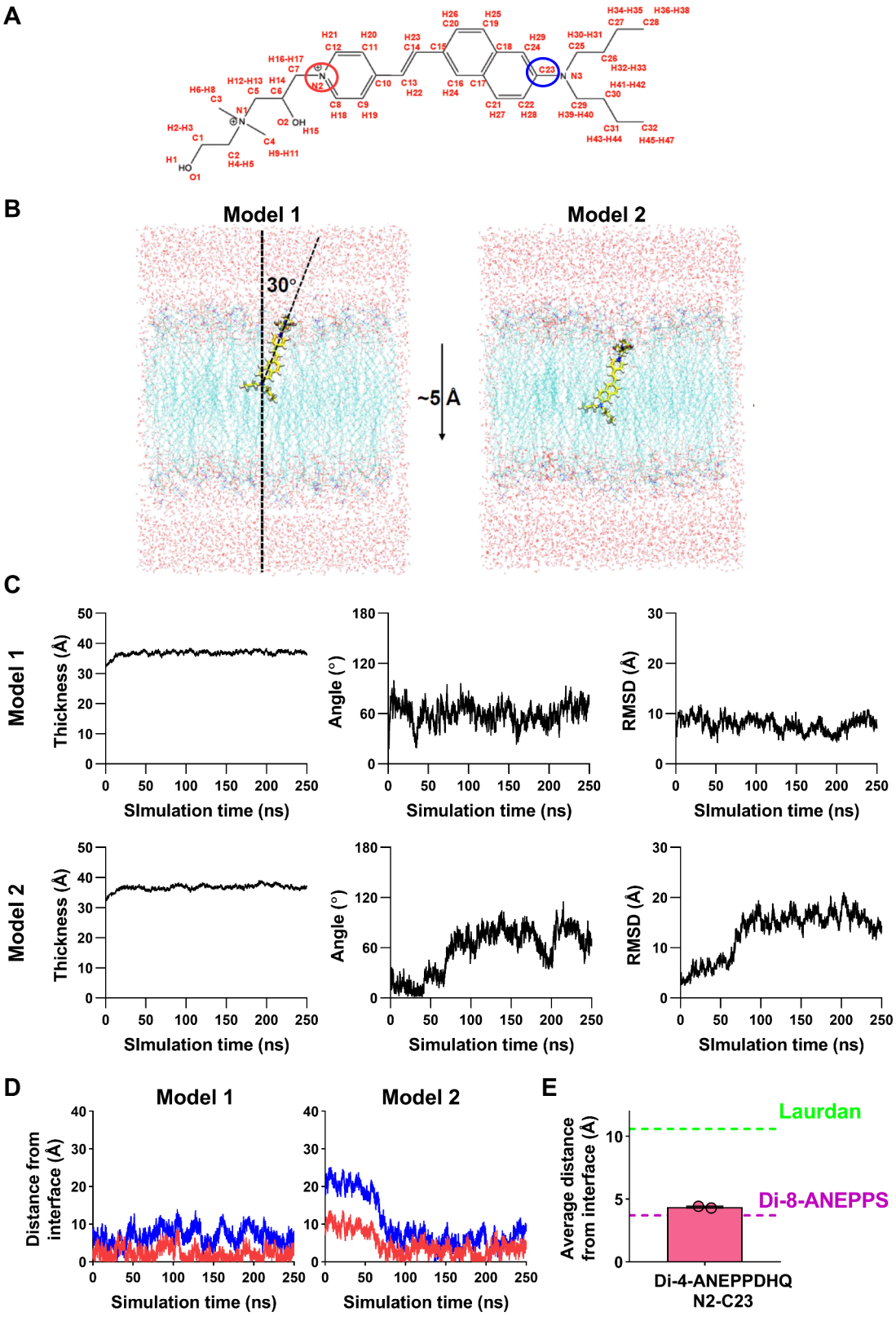

Figure 3. Membrane localization of the chromophore moiety of di-4-ANEPPDHQ. (A) Schematic structure of di-4-ANEPPDHQ displayed with the name of each atom labeled in red. The atoms selected for further analysis are circled with the red and blue circles showing the boundaries of the chromophore groups. (B) Di-4-ANEPPDHQ was embedded into a pre-equilibrated lipid bilayer composed of 1-palmitoyl-2-oleoyl-*sn*-glycero-3-phosphocholine (POPC) with the initial orientation of the fluorophore having a 30° angle to the membrane normal with the tilt angle to membrane normal measured based on atoms N2 and N3, and the dye localized at two different initial depths shifted by 5 Å (model 1 and model 2). The tilt angle is labeled in model 1. (C) Membrane thickness values measured between the P atoms in the top and bottom layers, tilt angles to the membrane normal, and positional RMSDs of the heavy atoms of the dye were plotted as a function of simulation time during the course of the MD simulation and demonstrate the overall stability of the system. (D) Distances of the N2 (red) and C23 (blue) atoms at the two opposing edges of

https://doi.org/10.1021/acs.jpclett.6c00048
J. Phys. Chem. Lett. 2026, 17, 4723−4731

Figure 3. continued

the chromophore moiety of di-4-ANEPPDHQ were calculated to the membrane surface defined as the position of the P atoms in phospholipids and plotted as a function of simulation time. (E) Mean positions of the selected atom pairs were calculated in the last 100 ns intervals of simulations and compared with those of atoms at the two opposing edges of the sensor moieties of Laurdan and di-8-ANEPPS determined in our previous study.[13]

DHC, and 6KC. No statistically significant correlation was found between generalized polarization values of di-4-ANEPPDHQ and Laurdan (Figure 2A). On the contrary, very strong, statistically significant positive correlation was seen between di-4-ANEPPDHQ generalized polarization and the di-8-ANEPPS excitation ratio (Figure 2B). This supports the hypothesis that in contrast to the widespread belief that both di-4-ANEPPDHQ and Laurdan share the same solvatochromic sensing mechanism, di-4-ANEPPDHQ cannot be considered a perfect alternative of Laurdan and suggests that the information provided by the dye in fact resembles much more closely that gained with di-8-ANEPPS, a probe with a presumably distinct sensing mechanism, electrochromism.

To investigate why the results obtained with di-4-ANEPPDHQ correlate more strongly with those of di-8-ANEPPS than with those of Laurdan, we examined the membrane localization of di-4-ANEPPDHQ using MD simulations following the positions of its heavy atoms (Figure 3A). We embedded the dye into a 1-palmitoyl-2-oleoyl-*sn*-glycero-3-phosphocholine (POPC) lipid bilayer at two different initial depths, model 1 and model 2, with the latter shifted 5 Å toward the bilayer center (Figure 3B). Overall, time-dependent examination of membrane thickness measured between the P atoms in two leaflets, tilt angles of the dye to membrane normal, and positional RMSDs of heavy atoms of the probe suggested that the system gained and maintained stability during the simulations (Figure 3C). We also followed time-dependent changes in the distance of N2 and C23 atoms at the two opposing edges of the chromophore moiety from the P atoms of phospholipids at the proximal interface (Figure 3D). Subsequently, we calculated the average position of the selected atoms in the last 100 ns interval of each simulation (Figure 3E). We found that the chromophore moiety was localized, on average, 4.4 Å from the membrane−water interface, which was much closer to the average depth localization of the sensor moiety of di-8-ANEPPS than to Laurdan, the two latter values determined in our previous study with identical simulation methods and conditions (3.7 and 10.6 Å, respectively).[13] Notably, the two simulations, although the fluorophore was positioned at different initial depths, yet yielded similar results since, after approximately 80 ns, localization of the dye in model 2 converged to that in model 1, and the trajectories became essentially indistinguishable for the remainder of the simulation time, which further supports our conclusions. Altogether, our MD simulations provided an explanation for our experimental results, showing that data gained with di-4-ANEPPDHQ are much more similar to those of di-8-ANEPPS rather than Laurdan. That is, the sensor moiety of di-4-ANEPPDHQ lies much closer to the membrane−water interface than that of Laurdan.

Both experimental and MD simulation data obtained in this study suggest that di-4-ANEPPDHQ is not an ideal alternative for Laurdan. In fact, the information provided by the two dyes is complementary rather than equivalent. Di-4-ANEPPDHQ was originally synthesized as a fluorophore having the same chromophore as potentiometric di-8-ANEPPS and the quaternary ammonium headgroup (DHQ) of the dienylstyryl-pyridinium dye RH795 with good water solubility and photostability, a low degree of internalization, and excitation falling in the range of standard microscope setups.[23] Its emission spectrum was demonstrated to undergo a notable blue-shift in cholesterol-enriched liquid-ordered model bilayers and lipid rafts of living cells, as well, making it a "phase-sensitive" probe, which was suggested to include both solvatochromic and electric field-dependent, electrochromic components. However, the former was deemed to provide a larger contribution to the observed spectral response.[22] Based on this assumption, di-4-ANEPPDHQ became widely known as a polarity-sensitive solvatochromic probe. In accordance, most studies simultaneously examining Laurdan, the prototypical solvatochromic dye, and di-4-ANEPPDHQ yielded similar results, and therefore, di-4-ANEPPDHQ became a generally accepted Laurdan alternative and information obtained with the two fluorophores was considered equivalent.[19,24−28] However, a thorough analysis of their steady state and time-resolved spectra in different solvents and phase-separated cell-derived giant plasma membrane vesicles suggested that distinct underlying mechanisms lay behind their spectral changes and thus the two fluorophores may report on different physicochemical membrane properties. The authors proposed that while changes in the general polarization of Laurdan are completely consistent with the typical solvent dipolar relaxation process, those of di-4-ANEPPDHQ may involve multiple mechanisms, including an electrochromic response.[32] Similar measurements performed in nanodiscs and liposomes also argued against the fully solvatochromic mechanism of the dye.[31]

Due to the inconsistent terminology of membrane biophysics in general and the only partially elucidated environment-sensing mechanism of di-4-ANEPPDHQ in particular, the interpretation of results obtained with the dye seems a bit confusing. A large fraction of recent studies attribute changes reported by the dye in simple terms and somewhat ambiguously to "membrane order"[49−52] or "lipid packing"[53−55] without addressing further details. When specified, "polarity-sensitive" di-4-ANEPPDHQ was most commonly suggested to report on membrane hydration;[29,30] however, "fluidity" and "rigidity" are also commonly used terms to interpret results gained with the probe.[56−60] Di-4-ANEPPDHQ was also described recently as a "voltage-sensitive" dye characterizing "membrane fluidity".[61] Furthermore, the depth localization of the probe and its relationship with the environmental sensitivity are not discussed in these studies. Based on our results, di-4-ANEPPDHQ reports on the molecular organization of membrane layers in the vicinity of the membrane−water boundary and, therefore, can be considered as a rather superficial probe, just like the structurally related di-8-ANEPPS, and in contrast with Laurdan that is located much closer to the hydrophobic core and thus can be considered as a deep probe. Both experimental evidence and MD simulation evidence presented in the study support the idea that di-4-ANEPPDHQ is not a substitute but rather a

https://doi.org/10.1021/acs.jpclett.6c00048
J. Phys. Chem. Lett. 2026, 17, 4723−4731

complementary tool for Laurdan. Our data may also imply that the classification of environment-sensitive dyes should be based on depth localization rather than the exact and often not fully understood molecular sensing mechanism. Moreover, the membrane structure cannot be thoroughly described without a combination of dyes reporting on distinct layers at different depths.

Furthermore, our results extend previous sporadic studies demonstrating incongruent changes in membrane structure in response to alterations in levels of certain sterols at different depths of bilayers.[10−12] The three sterols applied in the study, cholesterol, 7-dehydrocholesterol, and 6-ketocholestanol, albeit having subtle differences in their chemical structures, induce distinct alterations in membrane layers at different depths and hence can be used as experimental tools to elucidate modulatory effects exerted by the bulk membrane structure on transmembrane proteins. Alterations in bulk membrane organization were previously shown to affect a variety of proteins, including receptor tyrosine kinases, G protein-coupled receptors, ion channels, and ATP-driven pumps, through hydrophobic mismatch, elastic coupling, or interactions between the dipole potential-associated electric field and charged or polar amino acid residues.[2,5,6,8,9,62,63] Investigating changes in membrane structure and their roles in modulating protein activities and thus cellular functions may be crucially relevant. Such studies could help explore novel routes of membrane lipid therapy aimed at correcting membrane composition and structure in diseases associated with altered membrane lipid levels, such as metabolic disorders, lysosomal storage diseases, neurodegenerative diseases, and various tumors.[6,64,65]

Limitations of the simulations in the current study include the use of pure POPC bilayers instead of complex, sterol-containing ones, which would better mimic real cellular membranes, to ensure comparability with prior studies examining the localization of environment-sensitive fluorophores.[66−71] Moreover, Laurdan can assume an "elongated" or an "L-shaped/bent" conformation in the membrane,[72] and the distribution between the two conformers may also contribute to its environmental sensitivity.[73,74] Therefore, it cannot be considered a simple stick standing as a purely solvatochromic reporter in the membrane; it may rather have a phase-dependent molecular rotor behavior, as well.[75−77] However, as a simplification in our prior comparative analysis, we modeled only the elongated form that, as recent studies demonstrated, may predominate in biological bilayers.[78] In the experimental part of our work, we investigated the effects of sterols only on the generalized polarization of di-4-ANEPPDHQ. While this parameter is most commonly examined when the fluorophore is used,[22,24,29,32,61,79] other properties could also be measured, such as lifetime,[25,80−82] anisotropy,[83] or time-resolved emission and relaxation dynamics.[31,32] Furthermore, while the utilized sterols carry both experimental and biological relevance, no systematic analysis of various lipid classes was performed in our measurements. Nevertheless, our strongly congruent experimental and computational results strongly support the relevance of the functional distinction between di-4-ANEPPDHQ and Laurdan.

In summary, using spectrofluorometry and confocal microscopy, we demonstrate here that different but structurally similar sterols induce distinct changes in the generalized polarization of the supposedly solvatochromic environment-sensitive di-4-ANEPPDHQ fluorophore, a proposed functional analogue of Laurdan, the founding member of solvatochromic probes. Somewhat surprisingly, these alterations exhibited no statistically significant correlation with Laurdan generalized polarization values but, contrastingly, showed excellent and significant positive correlations with changes in the dipole potential-dependent excitation ratios of the electrochromic di-8-ANEPPS fluorophore. Our MD simulations demonstrated that this may be related to the depth localizations of the fluorophores since the sensor moiety of di-4-ANEPPDHQ was found in the vicinity of the membrane−water interface, much closer to that of di-8-ANEPPS than that of Laurdan, with the latter being localized much deeper in the hydrophobic core regions. Altogether, our findings imply that the information provided by di-4-ANEPPDHQ may be complementary rather than equivalent to that obtained with the solvatochromic Laurdan and resembles much more closely that obtained with voltage-sensing di-8-ANEPPS. Therefore, conclusions based on the general assumption that di-4-ANEPPDHQ and Laurdan are functionally equivalent should be treated with caution. Furthermore, based on our results, the classification of environment-sensitive fluorophores should include their depth localization in the bilayers rather than focusing solely on the mechanism of sensation, and the membrane biophysical terms should be more unambiguously used when interpreting results gained with these dyes.

■ ASSOCIATED CONTENT

Supporting Information

The Supporting Information is available free of charge at https://pubs.acs.org/doi/10.1021/acs.jpclett.6c00048.

Experimental section with a detailed description of the utilized cell culture and treatments, examination of spectral changes of di-4-ANEPPDHQ using spectrofluorometry, quantification of the generalized polarization of di-4-ANEPPDHQ using confocal microscopy, molecular dynamics simulations, and statistical analysis (PDF)

■ AUTHOR INFORMATION

Corresponding Authors

Florina Zakany − *Department of Biophysics and Cell Biology, Faculty of Medicine, University of Debrecen and MTA Centre of Excellence, Hungarian Academy of Sciences, Debrecen H-4032, Hungary*; Email: florina.zakany@med.unideb.hu

Tamas Kovacs − *Department of Biophysics and Cell Biology, Faculty of Medicine, University of Debrecen and MTA Centre of Excellence, Hungarian Academy of Sciences, Debrecen H-4032, Hungary*; orcid.org/0000-0002-1084-9847; Email: kovacs.tamas@med.unideb.hu

Authors

Rosemary Chandrakanthi Kothalawala − *Department of Biophysics and Cell Biology, Faculty of Medicine, University of Debrecen and MTA Centre of Excellence, Hungarian Academy of Sciences, Debrecen H-4032, Hungary*

Csenge Makay − *Department of Biophysics and Cell Biology, Faculty of Medicine, University of Debrecen and MTA Centre of Excellence, Hungarian Academy of Sciences, Debrecen H-4032, Hungary*

Lajos Szente − *CycloLab Cyclodextrin R&D Laboratory Ltd., Budapest H-1097, Hungary*

https://doi.org/10.1021/acs.jpclett.6c00048
J. Phys. Chem. Lett. 2026, 17, 4723−4731

Zoltan Varga − *Department of Biophysics and Cell Biology, Faculty of Medicine, University of Debrecen and MTA Centre of Excellence, Hungarian Academy of Sciences, Debrecen H-4032, Hungary;* orcid.org/0000-0003-1892-6840

Gyorgy Panyi − *Department of Biophysics and Cell Biology, Faculty of Medicine, University of Debrecen and MTA Centre of Excellence, Hungarian Academy of Sciences, Debrecen H-4032, Hungary;* orcid.org/0000-0001-6227-3301

Peter Nagy − *Department of Biophysics and Cell Biology, Faculty of Medicine, University of Debrecen and MTA Centre of Excellence, Hungarian Academy of Sciences, Debrecen H-4032, Hungary;* orcid.org/0000-0002-7466-805X

Complete contact information is available at: https://pubs.acs.org/10.1021/acs.jpclett.6c00048

Author Contributions

R.C.K.: investigation, formal analysis, visualization, and writing of the original draft. C.M.: investigation, formal analysis, and writing of the original draft. L.S.: methodology and review and editing. Z.V.: supervision, funding, and review and editing. G.P.: supervision, funding, and review and editing. P.N.: methodology, formal analysis, funding, visualization, and review and editing. F.Z.: conceptualization, investigation, methodology, formal analysis, visualization, funding, writing of the original draft, and review and editing. T.K.: conceptualization, investigation, methodology, formal analysis, visualization, supervision, project administration, funding, writing of the original draft, and review and editing. All authors reviewed the final manuscript and provided inputs. The manuscript was written through contributions of all authors. All authors have given approval to the final version of the manuscript.

Funding

This research was funded by the Hungarian National Research, Development and Innovation Office (OTKA FK143400, STARTING 153195, T.K.; OTKA FK146740, F.Z.; OTKA K138075 and ANN133421, P.N.; OTKA K132906, Z.V.; and OTKA K143071, G.P.). This project was supported by the EKÖP-24-2-DE-298 (R.C.K.) University Research Scholarship Program of the Ministry for Culture and Innovation from the source of the National Research, Development and Innovation Fund and by the János Bolyai Research Scholarship of the Hungarian Academy of Sciences (BO/00392/23, T.K.; BO/00676/24, F.Z.). This research work was conducted with the support of the National Academy of Scientist Education Program of the National Biomedical Foundation under the sponsorship of the Hungarian Ministry of Culture and Innovation (R.C.K.). Supported by the University of Debrecen Program for Scientific Publication. Project 2024-1.2.3-HU-RIZONT-2024−00099 has been implemented with the support provided by the Ministry of Culture and Innovation of Hungary from the National Research, Development and Innovation Fund, financed under the 2024-1.2.3-HU-RIZONT funding scheme.

Notes

The authors declare the following competing financial interest(s): L.S. is currently employed by the Cyclodextrin R&D Laboratory Ltd. The remaining authors declare no conflict of interest. The funders had no role in the writing of the manuscript.

■ ACKNOWLEDGMENTS

The authors are thankful for the expert technical assistance of Rita Utasi-Szabo.

■ ABBREVIATIONS

6KC, 6-ketocholestanol; 7DHC, 7-dehydrocholesterol; CD, cyclodextrin; CHOL, cholesterol; di-8-ANEPPS, 4-(2-[6-(dioctylamino)-2-naphthalenyl]ethenyl)-1-(3-sulfopropyl)-pyridinium inner salt; Laurdan, 6-dodecanoyl-*N*,*N*-dimethyl-2-naphthylamine; MβCD, randomly methylated β-cyclodextrin; POPC, 1-palmitoyl-2-oleoyl-*sn*-glycero-3-phosphocholine; PY3174, (4-[2-(6-dibutylamino-5-fluoronaphthalen-2-yl)-vinyl]-1-(3-triethylammoniopropyl)pyridinium dibromide; TMA-DPH, 4′-(trimethylammonio)diphenylhexatriene

■ REFERENCES

(1) Levental, I.; Lyman, E. Regulation of membrane protein structure and function by their lipid nano-environment. *Nat. Rev. Mol. Cell Biol.* **2023**, *24* (2), 107−22.

(2) Zakany, F.; Kovacs, T.; Panyi, G.; Varga, Z. Direct and indirect cholesterol effects on membrane proteins with special focus on potassium channels. *Biochim Biophys Acta Mol. Cell Biol. Lipids.* **2020**, *1865* (8), 158706.

(3) Klymchenko, A. S. Solvatochromic and Fluorogenic Dyes as Environment-Sensitive Probes: Design and Biological Applications. *Acc. Chem. Res.* **2017**, *50* (2), 366−75.

(4) Klymchenko, A. S. Fluorescent Probes for Lipid Membranes: From the Cell Surface to Organelles. *Acc. Chem. Res.* **2023**, *56* (1), 1−12.

(5) Kovacs, T.; Nagy, P.; Panyi, G.; Szente, L.; Varga, Z.; Zakany, F. Cyclodextrins: Only Pharmaceutical Excipients or Full-Fledged Drug Candidates? *Pharmaceutics* **2022**, *14* (12), 2559.

(6) Kovacs, T.; Zakany, F.; Nagy, P. It Takes More than Two to Tango: Complex, Hierarchal, and Membrane-Modulated Interactions in the Regulation of Receptor Tyrosine Kinases. *Cancers* **2022**, *14* (4), 944.

(7) O'Shea, P. Intermolecular interactions with/within cell membranes and the trinity of membrane potentials: kinetics and imaging. *Biochem. Soc. Trans.* **2003**, *31* (5), 990−6.

(8) Wang, L. Measurements and implications of the membrane dipole potential. *Annu. Rev. Biochem.* **2012**, *81*, 615−35.

(9) Zakany, F.; Mandity, I. M.; Varga, Z.; Panyi, G.; Nagy, P.; Kovacs, T. Effect of the Lipid Landscape on the Efficacy of Cell-Penetrating Peptides. *Cells* **2023**, *12* (13), 1700.

(10) Batta, G.; Karpati, L.; Henrique, G. F.; Toth, G.; Tarapcsak, S.; Kovacs, T.; Zakany, F.; Mándity, I. M.; Nagy, P. Statin-boosted cellular uptake and endosomal escape of penetratin due to reduced membrane dipole potential. *Br. J. Pharmacol.* **2021**, *178*, 3667.

(11) Cs. Szabo, B.; Szabo, M.; Nagy, P.; Varga, Z.; Panyi, G.; Kovacs, T.; Zakany, F. Novel insights into the modulation of the voltage-gated potassium channel K(V)1.3 activation gating by membrane ceramides. *J. Lipid Res.* **2024**, *65* (8), 100596.

(12) Zakany, F.; Szabo, M.; Batta, G.; Karpati, L.; Mandity, I. M.; Fulop, P.; et al. An omega-3, but Not an omega-6 Polyunsaturated Fatty Acid Decreases Membrane Dipole Potential and Stimulates Endo-Lysosomal Escape of Penetratin. *Front Cell Dev Biol.* **2021**, *9*, 647300.

(13) Zakany, F.; Kothalawala, R. C.; Pavela, O.; Szente, L.; Varga, Z.; Panyi, G. The many layers of membrane biophysics: Environment-sensitive fluorophores report on structural organization of biological membranes at various depths. *Anal. Chem.*, in press.

(14) Parasassi, T.; De Stasio, G.; Ravagnan, G.; Rusch, R. M.; Gratton, E. Quantitation of lipid phases in phospholipid vesicles by the generalized polarization of Laurdan fluorescence. *Biophys. J.* **1991**, *60* (1), 179−89.

(15) Gunther, G.; Malacrida, L.; Jameson, D. M.; Gratton, E.; Sanchez, S. A. LAURDAN since Weber: The Quest for Visualizing Membrane Heterogeneity. *Acc. Chem. Res.* **2021**, *54* (4), 976−87.
(16) Batta, G.; Soltesz, L.; Kovacs, T.; Bozo, T.; Meszar, Z.; Kellermayer, M.; et al. Alterations in the properties of the cell membrane due to glycosphingolipid accumulation in a model of Gaucher disease. *Sci. Rep.* **2018**, *8* (1), 157.
(17) Kovacs, T.; Sohajda, T.; Szente, L.; Nagy, P.; Panyi, G.; Varga, Z.; et al. Cyclodextrins Exert a Ligand-like Current Inhibitory Effect on the K(V)1.3 Ion Channel Independent of Membrane Cholesterol Extraction. *Front Mol. Biosci.* **2021**, *8*, 735357.
(18) Parasassi, T.; Gratton, E.; Yu, W. M.; Wilson, P.; Levi, M. Two-photon fluorescence microscopy of laurdan generalized polarization domains in model and natural membranes. *Biophys. J.* **1997**, *72* (6), 2413−29.
(19) Sezgin, E.; Waithe, D.; Bernardino de la Serna, J.; Eggeling, C. Spectral imaging to measure heterogeneity in membrane lipid packing. *Chemphyschem.* **2015**, *16* (7), 1387−94.
(20) Varela, A. R.; Ventura, A. E.; Carreira, A. C.; Fedorov, A.; Futerman, A. H.; Prieto, M.; et al. Pathological levels of glucosylceramide change the biophysical properties of artificial and cell membranes. *Phys. Chem. Chem. Phys.* **2017**, *19* (1), 340−6.
(21) Gaus, K.; Zech, T.; Harder, T. Visualizing membrane microdomains by Laurdan 2-photon microscopy. *Mol. Membr. Biol.* **2006**, *23* (1), 41−8.
(22) Jin, L.; Millard, A. C.; Wuskell, J. P.; Dong, X.; Wu, D.; Clark, H. A.; et al. Characterization and application of a new optical probe for membrane lipid domains. *Biophys. J.* **2006**, *90* (7), 2563−75.
(23) Obaid, A. L.; Loew, L. M.; Wuskell, J. P.; Salzberg, B. M. Novel naphthylstyryl-pyridium potentiometric dyes offer advantages for neural network analysis. *J. Neurosci Methods.* **2004**, *134* (2), 179−90.
(24) Owen, D. M.; Rentero, C.; Magenau, A.; Abu-Siniyeh, A.; Gaus, K. Quantitative imaging of membrane lipid order in cells and organisms. *Nat. Protoc.* **2012**, *7* (1), 24−35.
(25) Owen, D. M.; Williamson, D. J.; Magenau, A.; Gaus, K. Sub-resolution lipid domains exist in the plasma membrane and regulate protein diffusion and distribution. *Nat. Commun.* **2012**, *3*, 1256.
(26) Alvarez-Guaita, A.; Vila de Muga, S.; Owen, D. M.; Williamson, D.; Magenau, A.; Garcia-Melero, A.; et al. Evidence for annexin A6-dependent plasma membrane remodelling of lipid domains. *Br. J. Pharmacol.* **2015**, *172* (7), 1677−90.
(27) Dinic, J.; Biverstahl, H.; Maler, L.; Parmryd, I. Laurdan and di-4-ANEPPDHQ do not respond to membrane-inserted peptides and are good probes for lipid packing. *Biochim. Biophys. Acta* **2011**, *1808* (1), 298−306.
(28) Roche, Y.; Gerbeau-Pissot, P.; Buhot, B.; Thomas, D.; Bonneau, L.; Gresti, J.; et al. Depletion of phytosterols from the plant plasma membrane provides evidence for disruption of lipid rafts. *FASEB J.* **2008**, *22* (11), 3980−91.
(29) Panconi, L.; Euchner, J.; Tashev, S. A.; Makarova, M.; Herten, D. P.; Owen, D. M.; et al. Mapping membrane biophysical nano-environments. *Nat. Commun.* **2024**, *15* (1), 9641.
(30) Sezgin, E.; Schneider, F.; Zilles, V.; Urbancic, I.; Garcia, E.; Waithe, D.; et al. Polarity-Sensitive Probes for Superresolution Stimulated Emission Depletion Microscopy. *Biophys. J.* **2017**, *113* (6), 1321−30.
(31) Chmielinska, A.; Stepien, P.; Bonarek, P.; Girych, M.; Enkavi, G.; Rog, T.; et al. Can di-4-ANEPPDHQ reveal the structural differences between nanodiscs and liposomes? *Biochim Biophys Acta Biomembr.* **2021**, *1863* (9), 183649.
(32) Amaro, M.; Reina, F.; Hof, M.; Eggeling, C.; Sezgin, E. Laurdan and Di-4-ANEPPDHQ probe different properties of the membrane. *J. Phys. D Appl. Phys.* **2017**, *50* (13), 134004.
(33) Chakraborty, S.; Doktorova, M.; Molugu, T. R.; Heberle, F. A.; Scott, H. L.; Dzikovski, B.; et al. How cholesterol stiffens unsaturated lipid membranes. *Proc. Natl. Acad. Sci. U. S. A.* **2020**, *117* (36), 21896−905.
(34) de Santis, A.; Scoppola, E.; Ottaviani, M. F.; Koutsioubas, A.; Barnsley, L. C.; Paduano, L.; et al. Order vs. Disorder: Cholesterol and Omega-3 Phospholipids Determine Biomembrane Organization. *Int. J. Mol. Sci.* **2022**, *23* (10), 5322.
(35) Ma, Y.; Benda, A.; Kwiatek, J.; Owen, D. M.; Gaus, K. Time-Resolved Laurdan Fluorescence Reveals Insights into Membrane Viscosity and Hydration Levels. *Biophys. J.* **2018**, *115* (8), 1498−508.
(36) Davis, S.; Davis, B. M.; Richens, J. L.; Vere, K. A.; Petrov, P. G.; Winlove, C. P.; et al. alpha-Tocopherols modify the membrane dipole potential leading to modulation of ligand binding by P-glycoprotein. *J. Lipid Res.* **2015**, *56* (8), 1543−50.
(37) Haldar, S.; Kanaparthi, R. K.; Samanta, A.; Chattopadhyay, A. Differential effect of cholesterol and its biosynthetic precursors on membrane dipole potential. *Biophys. J.* **2012**, *102* (7), 1561−9.
(38) Kovacs, T.; Batta, G.; Zakany, F.; Szollosi, J.; Nagy, P. The dipole potential correlates with lipid raft markers in the plasma membrane of living cells. *J. Lipid Res.* **2017**, *58* (8), 1681−91.
(39) Sarkar, P.; Rao, B. D.; Chattopadhyay, A. Cell Cycle Dependent Modulation of Membrane Dipole Potential and Neurotransmitter Receptor Activity: Role of Membrane Cholesterol. *ACS Chem. Neurosci.* **2020**, *11* (18), 2890−9.
(40) Kovacs, T.; Kurtan, K.; Varga, Z.; Nagy, P.; Panyi, G.; Zakany, F. Veklury(R) (remdesivir) formulations inhibit initial membrane-coupled events of SARS-CoV-2 infection due to their sulfobutylether-beta-cyclodextrin content. *Br. J. Pharmacol.* **2023**, *180* (16), 2064−84.
(41) Szabo, M.; Cs. Szabo, B.; Kurtan, K.; Varga, Z.; Panyi, G.; Nagy, P.; et al. Look Beyond Plasma Membrane Biophysics: Revealing Considerable Variability of the Dipole Potential Between Plasma and Organelle Membranes of Living Cells. *Int. J. Mol. Sci.* **2025**, *26* (3), 889.
(42) Shrivastava, S.; Paila, Y. D.; Dutta, A.; Chattopadhyay, A. Differential effects of cholesterol and its immediate biosynthetic precursors on membrane organization. *Biochemistry.* **2008**, *47* (20), 5668−77.
(43) Singh, P.; Haldar, S.; Chattopadhyay, A. Differential effect of sterols on dipole potential in hippocampal membranes: implications for receptor function. *Biochim. Biophys. Acta* **2013**, *1828* (3), 917−23.
(44) Clarke, R. J.; Kane, D. J. Optical detection of membrane dipole potential: avoidance of fluidity and dye-induced effects. *Biochim. Biophys. Acta* **1997**, *1323* (2), 223−39.
(45) Gross, E.; Bedlack, R. S., Jr.; Loew, L. M. Dual-wavelength ratiometric fluorescence measurement of the membrane dipole potential. *Biophys. J.* **1994**, *67* (1), 208−16.
(46) Kovacs, T.; Batta, G.; Hajdu, T.; Szabo, A.; Varadi, T.; Zakany, F.; et al. The Dipole Potential Modifies the Clustering and Ligand Binding Affinity of ErbB Proteins and Their Signaling Efficiency. *Sci. Rep.* **2016**, *6*, 35850.
(47) Zakany, F.; Pap, P.; Papp, F.; Kovacs, T.; Nagy, P.; Peter, M.; et al. Determining the target of membrane sterols on voltage-gated potassium channels. *Biochim Biophys Acta Mol. Cell Biol. Lipids.* **2019**, *1864* (3), 312−25.
(48) Zidovetzki, R.; Levitan, I. Use of cyclodextrins to manipulate plasma membrane cholesterol content: evidence, misconceptions and control strategies. *Biochim. Biophys. Acta* **2007**, *1768* (6), 1311−24.
(49) Asnacios, S.; Staneva, G.; Thon, G.; Vannier, F.; Carn, F.; Puff, N.; et al. Alzheimer's disease amyloid-beta affects membrane structure and mechanical properties of human neural progenitors. *J. Alzheimer's Dis.* **2026**, *109*, No. 633.
(50) Savoye, K.; Nieves, D. J.; Shirgill, S.; Lewis, A.; Spill, F.; Owen, D. M. Measuring the similarity of single-molecule localization microscopy derived marked point clouds. *Biophys. J.* **2025**, *124* (18), 2931−40.
(51) Lv, X.; Zhang, C.; Cui, S.; Xu, X.; Wang, L.; Li, J.; et al. Assembly of pathway enzymes by engineering functional membrane microdomain components for improved N-acetylglucosamine synthesis in Bacillus subtilis. *Metab Eng.* **2020**, *61*, 96−105.
(52) Wu, Z.; Fan, C.; Man, Y.; Zhang, Y.; Li, R.; Li, X.; et al. Both Clathrin-Mediated and Membrane Microdomain-Associated Endocytosis Contribute to the Cellular Adaptation to Hyperosmotic Stress in Arabidopsis. *Int. J. Mol. Sci.* **2021**, *22* (22), 12534.

https://doi.org/10.1021/acs.jpclett.6c00048
J. Phys. Chem. Lett. 2026, 17, 4723−4731

(53) Lorent, J. H.; Levental, K. R.; Ganesan, L.; Rivera-Longsworth, G.; Sezgin, E.; Doktorova, M.; et al. Plasma membranes are asymmetric in lipid unsaturation, packing and protein shape. *Nat. Chem. Biol.* **2020**, *16* (6), 644−52.
(54) Hsu, W. Y.; Masuda, T.; Afonin, S.; Sakai, T.; Arafiles, J. V. V.; Kawano, K.; et al. Enhancing the activity of membrane remodeling epsin-peptide by trimerization. *Bioorg. Med. Chem. Lett.* **2020**, *30* (12), 127190.
(55) Murayama, T.; Masuda, T.; Afonin, S.; Kawano, K.; Takatani-Nakase, T.; Ida, H.; et al. Loosening of Lipid Packing Promotes Oligoarginine Entry into Cells. *Angew. Chem., Int. Ed. Engl.* **2017**, *56* (26), 7644−7.
(56) Romanova, N.; Sule, K.; Issler, T.; Hebrok, D.; Persicke, M.; Thevenod, F.; et al. Cadmium-cardiolipin disruption of respirasome assembly and redox balance through mitochondrial membrane rigidification. *J. Lipid Res.* **2025**, *66* (3), 100750.
(57) Anselmo, S.; Sancataldo, G.; Baiamonte, C.; Pizzolanti, G.; Vetri, V. Transportan 10 Induces Perturbation and Pores Formation in Giant Plasma Membrane Vesicles Derived from Cancer Liver Cells. *Biomolecules* **2023**, *13* (3), 492.
(58) Varyukhina, S.; Lamaziere, A.; Delaunay, J. L.; de Wreede, A.; Ayala-Sanmartin, J. The Ca(2+)- and phospholipid-binding protein Annexin A2 is able to increase and decrease plasma membrane order. *Biochim Biophys Acta Biomembr.* **2022**, *1864* (1), 183810.
(59) Salinas, M. L.; Fuentes, N. R.; Choate, R.; Wright, R. C.; McMurray, D. N.; Chapkin, R. S. AdipoRon Attenuates Wnt Signaling by Reducing Cholesterol-Dependent Plasma Membrane Rigidity. *Biophys. J.* **2020**, *118* (4), 885−97.
(60) Fernandez-Perez, E. J.; Sepulveda, F. J.; Peters, C.; Bascunan, D.; Riffo-Lepe, N. O.; Gonzalez-Sanmiguel, J.; et al. Effect of Cholesterol on Membrane Fluidity and Association of Abeta Oligomers and Subsequent Neuronal Damage: A Double-Edged Sword. *Front. Aging Neurosci.* **2018**, *10*, 226.
(61) Siniyeh, A. A.; Alshaer, W.; Elzogheir, N.; Al-Holi, M.; Alqudah, D. A.; Abuarqoub, D.; et al. Comparative analysis of RT-qPCR, flow cytometry, and Di-4-ANEPPDHQ fluorescence for distinguishing macrophages phenotypes. *Biochem Biophys Rep.* **2025**, *44*, 102225.
(62) Brown, M. F. Soft Matter in Lipid-Protein Interactions. *Annu. Rev. Biophys.* **2017**, *46*, 379−410.
(63) Richens, J. L.; Lane, J. S.; Bramble, J. P.; O'Shea, P. The electrical interplay between proteins and lipids in membranes. *Biochim. Biophys. Acta* **2015**, *1848* (9), 1828−36.
(64) Casares, D.; Escriba, P. V.; Rossello, C. A. Membrane Lipid Composition: Effect on Membrane and Organelle Structure, Function and Compartmentalization and Therapeutic Avenues. *Int. J. Mol. Sci.* **2019**, *20* (9), 2167.
(65) Escriba, P. V.; Busquets, X.; Inokuchi, J.; Balogh, G.; Torok, Z.; Horvath, I.; et al. Membrane lipid therapy: Modulation of the cell membrane composition and structure as a molecular base for drug discovery and new disease treatment. *Prog. Lipid Res.* **2015**, *59*, 38−53.
(66) Barucha-Kraszewska, J.; Kraszewski, S.; Ramseyer, C. Will C-Laurdan dethrone Laurdan in fluorescent solvent relaxation techniques for lipid membrane studies? *Langmuir.* **2013**, *29* (4), 1174−82.
(67) Bouquiaux, C.; Tonnele, C.; Castet, F.; Champagne, B. Second-Order Nonlinear Optical Properties of an Amphiphilic Dye Embedded in a Lipid Bilayer. A Combined Molecular Dynamics-Quantum Chemistry Study. *J. Phys. Chem. B* **2020**, *124* (11), 2101−9.
(68) do Canto, A.; Robalo, J. R.; Santos, P. D.; Carvalho, A. J. P.; Ramalho, J. P. P.; Loura, L. M. S. Diphenylhexatriene membrane probes DPH and TMA-DPH: A comparative molecular dynamics simulation study. *Biochim. Biophys. Acta* **2016**, *1858* (11), 2647−61.
(69) Osella, S.; Murugan, N. A.; Jena, N. K.; Knippenberg, S. Investigation into Biological Environments through (Non)linear Optics: A Multiscale Study of Laurdan Derivatives. *J. Chem. Theory Comput.* **2016**, *12* (12), 6169−81.
(70) Warshaviak, D. T.; Muellner, M. J.; Chachisvilis, M. Effect of membrane tension on the electric field and dipole potential of lipid bilayer membrane. *Biochim. Biophys. Acta* **2011**, *1808* (10), 2608−17.
(71) Youngworth, R.; Roux, B. Simulating the Voltage-Dependent Fluorescence of Di-8-ANEPPS in a Lipid Membrane. *J. Phys. Chem. Lett.* **2023**, *14* (36), 8268−76.
(72) Osella, S.; Smisdom, N.; Ameloot, M.; Knippenberg, S. Conformational Changes as Driving Force for Phase Recognition: The Case of Laurdan. *Langmuir.* **2019**, *35* (35), 11471−81.
(73) Bacalum, M.; Radu, M.; Osella, S.; Knippenberg, S.; Ameloot, M. Generalized polarization and time-resolved fluorescence provide evidence for different populations of Laurdan in lipid vesicles. *J. Photochem. Photobiol. B* **2024**, *250*, 112833.
(74) Knippenberg, S.; De, K.; Aisenbrey, C.; Bechinger, B.; Osella, S. Hydration- and Temperature-Dependent Fluorescence Spectra of Laurdan Conformers in a DPPC Membrane. *Cells* **2024**, *13* (15), 1232.
(75) Osella, S.; Knippenberg, S. Laurdan as a Molecular Rotor in Biological Environments. *ACS Appl. Bio Mater.* **2019**, *2* (12), 5769−78.
(76) Osella, S.; Knippenberg, S. The influence of lipid membranes on fluorescent probes' optical properties. *Biochim Biophys Acta Biomembr.* **2021**, *1863* (2), 183494.
(77) Osella, S.; Knippenberg, S. Photophysics in Biomembranes: Computational Insight into the Interaction between Lipid Bilayers and Chromophores. *Acc. Chem. Res.* **2024**, *57* (16), 2245−54.
(78) Lester, A.; Orlikowska-Rzeznik, H.; Krok, E.; Piatkowski, L. Laurdan Adopts Distinct, Phase-Specific Orientations in Lipid Membranes. *J. Phys. Chem. B* **2025**, *129* (25), 6233−40.
(79) Goossens, P.; Rodriguez-Vita, J.; Etzerodt, A.; Masse, M.; Rastoin, O.; Gouirand, V.; et al. Membrane Cholesterol Efflux Drives Tumor-Associated Macrophage Reprogramming and Tumor Progression. *Cell Metab.* **2019**, *29* (6), 1376−89.
(80) Owen, D. M.; Lanigan, P. M.; Dunsby, C.; Munro, I.; Grant, D.; Neil, M. A.; et al. Fluorescence lifetime imaging provides enhanced contrast when imaging the phase-sensitive dye di-4-ANEPPDHQ in model membranes and live cells. *Biophys. J.* **2006**, *90* (11), L80−2.
(81) Sputay, D.; Doktorova, M.; Chan, S. H.; Guo, E. H.; Wang, H. Y.; Lorent, J. H.; et al. Immune cell activation produces locally scrambled foci of plasma membrane lipids. *Faraday Discuss.* **2025**, *259* (0), 45−59.
(82) Ragaller, F.; Sjule, E.; Urem, Y. B.; Schlegel, J.; El, R.; Urbancic, D.; et al. Quantifying Fluorescence Lifetime Responsiveness of Environment-Sensitive Probes for Membrane Fluidity Measurements. *J. Phys. Chem. B* **2024**, *128* (9), 2154−67.
(83) Steele, H. B. B.; Sydor, M. J.; Anderson, D. S.; Holian, A.; Ross, J. B. A. Using Time-Resolved Fluorescence Anisotropy of di-4-ANEPPDHQ and F2N12S to Analyze Lipid Packing Dynamics in Model Systems. *J. Fluoresc.* **2019**, *29* (2), 347−52.

https://doi.org/10.1021/acs.jpclett.6c00048
J. Phys. Chem. Lett. 2026, 17, 4723−4731

Disorder in order-related membrane biophysical parameters: An in-depth analysis of di-4-ANEPPDHQ generalized polarization

Rosemary Chandrakanthi Kothalawala[a], *Csenge Makay*[a], *Lajos Szente*[b], *Zoltan Varga*[a], *Gyorgy Panyi*[a], *Peter Nagy*[a], *Florina Zakany*[a*], *Tamas Kovacs*[a*]

[a] Department of Biophysics and Cell Biology, Faculty of Medicine, University of Debrecen and MTA Centre of Excellence, Hungarian Academy of Sciences, Egyetem tér 1, Debrecen H-4032, Hungary

[b] CycloLab Cyclodextrin R&D Laboratory Ltd., Illatos u. 7., Budapest H-1097, Hungary

[*] florina.zakany@med.unideb.hu, kovacs.tamas@med.unideb.hu

Experimental Section

Cell Culture and Treatments

Chinese hamster ovary (CHO) cells obtained from the American Type Culture Collection (Manassas, VA) were grown according to their specifications. Cell were detached at a confluence of 80%–90% by trypsinization for spectrofluorometry, whereas the cells were grown on 8-well chambered coverglass (ibidi, Gräfelfing, Germany) for confocal microscopy. Before the measurements, cells were treated with 6-ketocholestanol (3β-hydroxy-5α-cholestan-6-one, 6KC) (Sigma Aldrich, St. Louis, MO), cholesterol (CHOL) (Sigma-Aldrich) or 7-dehydrocholesterol (7DHC) (Sigma-Aldrich) pre-complexed with methyl-beta-cyclodextrin (MβCD) (CycloLab Cyclodextrin R&D Laboratory, Budapest, Hungary) at sterol concentrations of 200 μM for 60 min at room temperature in normal Ringer's solution. Control samples were treated with the corresponding amounts of native MβCD.

Examination of Spectral Changes of Di-4-ANEPPDHQ Using Spectrofluorometry

Trypsinized control CHO cells and those treated with native or sterol-loaded MβCD complexes for 60 min were labeled with 5 μM di-4-ANEPPDHQ (Thermo Fisher Scientific, Waltham, MA) for 20 min at room temperature. After washing and resuspension at a concentration of 10^6/ml, fluorescence intensities were measured with a Fluorolog-3 spectrofluorometer (Horiba Jobin Yvon, Edison, NJ). The probe was excited at 488 nm and the emission spectrum was determined

between 500 nm and 750 nm with an increment of 1 nm using slits adjusted to 5 nm both on the excitation and emission sides. Generalized polarization (GP) of di-4-ANEPPDHQ fluorescence was calculated by integrating the measured intensities in two emission wavelength ranges between 500 and 570 nm (I_{blue}) and 660 and 735 nm (I_{red}) and according to the following formula:

$$GP = \frac{I_{blue} - I_{red}}{I_{blue} + I_{red}} \quad \text{(S1).}$$

Quantification of the Generalized Polarization of Di-4-ANEPPDHQ Using Confocal Microscopy

The GP of di-4-ANEPPDHQ in CHO cells, grown on 8-well chambered coverglass and treated and labeled as above, was quantified using an LSM880 confocal laser-scanning microscope (Carl Zeiss AG, Jena, Germany). Images were acquired at the midplane of cells using an excitation at 488 nm and detecting emitted fluorescence intensities in the wavelength ranges corresponding to I_{blue} and I_{red}, specified above. During quantitative image analysis performed in MATLAB (Mathworks, Natick, MA), images were segmented into membrane and nonmembrane pixels, which was followed by the identification of individual cells and calculation of the median value of di-4-ANEPPDHQ GP from the data of plasma membrane pixels for each individual cell after background subtraction using equation (1) as demonstrated in Figure 1C.

Molecular Dynamics Simulations

The structure of di-4-ANEPPDHQ was obtained from quantum mechanics (QM) optimized geometries and used for electrostatic potential (ESP) calculations. QM calculations were performed at the B3LYP/6-31G*//HF/6-31G* level of theory. The atomic partial charges were

derived with restrained electrostatic potential (RESP) methodology with a restraint weight of 0.01 from previous ESP calculations. GAFF force field parameters were used to describe the valence parameters. The di-4-ANEPPDHQ was embedded into a pre-equilibrated lipid bilayer composed of 1-palmitoyl-2-oleoyl-sn-glycero-3-phosphocholine (POPC) built with CHARMM-GUI at two different positions (Model 1 and Model 2 with the probe moved towards the center of the bilayer by 5 Å in the latter) with an initial tilt angle of approximately 30˚ relative to the membrane normal. The system was solvated in a TIP3P bilayer water shell and neutralized by adding chloride ions and, subsequently, 150 mM NaCl was added to simulate physiological salt concentration. The valence parameters of POPC were adopted from Lipid14.

Energy minimization was performed on the entire system for 1000 steps utilizing the steepest descent method and then 1000 steps employing the conjugate gradient method with a restrained of 100 kcal·mol^{-1}·Å^{-2} applied to the phospholipid head groups and dye heavy atoms. Then, the same optimization process was carried out, but with the restraint applied solely to the probe and the entire system was gradually heated to 300 K over 40 ps under the same restraint conditions. Subsequently, a 100-ps equilibration simulation was performed under the nPT ensemble at 300 K to balance the system density, using the CPU version of PMEMD from the AMBER22 software package with smaller restraints applied to the dye heavy atoms (10 kcal·mol^{-1}·Å^{-2}). All restraints were removed in 1-ns equilibration simulations to further optimize the system density, which were carried out with the GPU implementation of PMEMD. Finally, 250-ns production MD simulations were performed with generally stable fluorophore positions obtained within this time interval. Atomic coordinates of all atoms were recorded every 10 ps. The temperature and

pressure were controlled using the Langevin thermostat and the anisotropic Berendsen barostat, respectively. Bond lengths involving hydrogen atoms were constrained using the SHAKE algorithm, Van der Waals interactions were treated using a nonbonding cutoff of 10 Å, and electrostatic interactions were calculated with the particle mesh Ewald method.

The membrane thickness was measured based on the average distance between the P atoms in the upper and lower leaflets of bilayers. The tilt angle to membrane normal was determined based on N2 and N3 atoms, whereas the positional RMSD was calculated based on the heavy atoms of the dye. Distances of di-4-ANEPPDHQ to the interface were calculated between N2 and C23 atoms of di-4-ANEPPDHQ and the P atoms in phospholipids.

Statistical Analysis

Measured data are represented as mean ± SEM obtained from n independent samples containing approximately 100,000 cells for spectrofluorometry or n individual cells from five independent experiments for confocal microscopy, as indicated in figure legends. The p values were calculated by Tukey's HSD test carried out after significant differences were obtained for between-group effects in ANOVA. Differences were considered significant when $p < 0.05$ (*$p < 0.05$, **$p < 0.01$, ***$p < 0.001$, ****$p < 0.0001$).